IGF2BP3 promotes progression of colorectal cancer and mediates cetuximab resistance by stabilizing EGFR mRNA in an m6A-dependent mechanism

Hongli Jiao
Southern Medical University
Lijie Chen
Southern Medical University
Huiye Liu
Southern Medical University
Zhiyuan Xiao
Southern Medical University
Ting Qiu
Southern Medical University
Dan Zhang
Southern Medical University
Lingjie Zhang
Southern Medical University
Fangyi Han
Southern Medical University
Guojun Chen
Southern Medical University
Xuemei Xu
Southern Medical University
Jionghua Zhu
Southern Medical University
Shuyang Wang
Southern Medical University
Yanqing Ding
Southern Medical University
Yaping Ye (149941225@qq.com)
Southern Medical University

Research Article

Keywords: IGF2BP3, m6A modification, EGFR, cetuximab resistance, CRC

Posted Date: February 1st, 2022

DOI: https://doi.org/10.21203/rs.3.rs-1297958/v1

Abstract

Background: Insulin-like growth factor 2 mRNA-binding protein 3 (IGF2BP3), an RNA-binding protein, is associated with tumorigenesis and progression. However, the exact molecular mechanisms of IGF2BP3 in colorectal cancer (CRC) oncogenesis, progression, and drug resistance remain largely unclear.

Methods: Transcriptome-sequencing, bioinformatics analysis, Western blot, and immunohistochemistry were performed to evaluate the expression of IGF2BP3 in CRC. Gene enrichment analysis and qPCR were used to assess the downstream targets of IGF2BP3. The molecular mechanisms of IGF2BP3 on CRC progression were explored through RNA stability assay, m^6A dot-blot, luciferase reporter assay, and MeRIP assay. In vitro and in vivo experiments were conducted to investigate the effects of IGF2BP3 on oncogenesis, progression and sensitivity to cetuximab of CRC.

Results: IGF2BP3 was upregulated in CRC tissues. Clinically, elevated IGF2BP3 level was predictive of a poor prognosis. Functionally, IGF2BP3 enhanced CRC tumorigenesis and progression in vitro and in vivo. Mechanistically, IGF2BP3 promoted epidermal growth factor receptor (EGFR) mRNA stability and translation, then further activated the EGFR pathway by serving as a reader in an N6-methyladenosine (m^6A)-dependent manner by cooperating with METTL14. Furthermore, IGF2BP3 increases drug resistance of CRC cells to the EGFR-targeted antibody cetuximab.

Conclusions: IGF2BP3 upregulation serve as an important oncogene in the development of CRC. It stabilizes EGFR mRNA via an m^6A-dependent manner and further promotes CRC progression and drug resistance to cetuximab. Targeting IGF2BP3 and m^6A modification offers rational therapeutic targets in CRC patients.

Background

Colorectal cancer (CRC) was estimated to be the third most commonly diagnosed cancer and the second leading cause of cancer death worldwide in 2020 [1]. Despite the improved substantial diagnostic and therapeutic strategies, the incidence of CRC remains high. Moreover, CRC gradually presents the characteristics of younger onset age [2], higher degree of malignancy, and more drug resistance. Thus, understanding the molecular mechanisms of CRC initiation and progression is essential for early diagnoses and effective therapy.

Insulin-like growth factor 2 mRNA-binding proteins (IGF2BPs), including IGF2BP1/2/3, are RNA-binding proteins (RBPs) that serve as posttranscriptional regulatory factors for mRNA stability and translation [3]. Over the past few years, studies have increasingly documented the contribution of IGF2BPs to fundamental processes in cancer biology. Among them, IGF2BP3 has been implicated in various aspects of human tumor progression regulating cell growth, migration, and the response to drugs [4]. IGF2BP3 has been explicated to be upregulated and play a potential oncogenic role in various tumor types, such as bladder cancer [5], lung cancer [6], gastric cancer [7], etc. Furthermore, IGF2BP3 has been identified as a

promising biomarker in different cancers including colon cancer [8, 9]. However, the molecular mechanism of IGF2BP3 in CRC remains largely unclear.

Epidermal growth factor receptor (EGFR), also known as ERBB1 or HER1, belongs to the ERBB family of cell-surface receptor tyrosine kinases. Abnormal, enhanced expression of EGFR triggers a series of intracellular signals that ultimately lead to the proliferation of cancer cells, induction of angiogenesis, and metastasis [10]. Although EGFR-targeted antibodies cetuximab and panitumumab have provided substantial benefits to patients with advanced cancer, the clinical efficacy is limited by the intrinsic and acquired resistance [11]. Understanding the molecular bases of resistance to EGFR blockade in CRC is therefore crucial.

As the most abundant mRNA modification, N6-methyladenosine (m^6A) modification participates in almost all steps of RNA metabolism including mRNA translation, degradation, splicing, export, and folding, which result in alteration of target gene expression [12]. M^6A plays critical roles in multiple fundamental biological processes such as cell differentiation, tissue development, and tumorigenesis [3]. The abundance and effects of m^6A on RNA are determined by the dynamic interplay between its methyltransferases (writers), binding proteins (readers), and demethylases (erasers) [13]. In this regard, readers are those that can recognize and bind to m^6A sites and lead to different destinies of target RNA, including translation, mRNA stability, nuclear trafficking, microRNA binding, and RNA-protein interaction [14]. For the past few years, the role of M^6A in tumor evolution has become a hot topic in CRC.

In the current study, we identified the oncogenic role of IGF2BP3. We found that IGF2BP3 was highly expressed in CRC, and upregulation of IGF2BP3 was associated with poor prognosis of CRC patients. Overexpression of IGF2BP3 enhanced CRC tumorigenesis and progression in vitro and in vivo. We demonstrated EGFR as a target gene of IGF2BP3 and that IGF2BP3 regulated EGFR expression by serving as a reader to stabilize m^6A-modified EGFR mRNA. In addition, we provided evidence that IGF2BP3 was associated with drug resistance of EGFR-targeted antibodies cetuximab in CRC.

Materials And Methods

Clinical samples

Paraffin samples of 67 CRC tissues with complete clinical data were obtained from Nanfang Hospital, Southern Medical University. A total of 47 CRC tissues and adjacent normal mucosa tissues were also collected from CRC patients undergoing standard resection, without chemotherapy or radiotherapy immunotherapy, at Nanfang Hospital. All specimens were histopathologically confirmed by at least 2 pathologists and obtained with informed consent. This study was approved by Southern Medical University Institutional Board (Guangzhou, China).

Cell culture and treatment

The human CRC cell lines SW620, LS174T, SW480, HCT15, LOVO, SW837, HT29, HCT116, Colo205, RKO, and CaCO2 were obtained from the American Type Culture Collection (ATCC). SW620 and HT29 cells were cultured in DMEM medium (Gibco) with 10% FBS (Gibco) at 37°C with 5% CO2. SW480, Colo205, Ls174t, HCT116, LoVo, HCT15, RKO, and CaCO2 cells were cultured in RPMI 1640 medium (Gibco) with 10% FBS (Gibco) at 37°C with 5% CO2. All these cell lines were routinely authenticated for purity and being infection-free.

Quantitative real-time PCR (qRT-PCR)

Total RNA was isolated from CRC tissues and cell lines using Trizol reagent (Invitrogen). 1μg total RNA was reverse transcribed into cDNA by PrimeScript RT reagent Kit (Takara). The acquired cDNAs were used as templates for quantitative real-time PCR analysis using ChamQTM Universal SYBR Q-PCR Master Mix (Vazyme). The relative RNA expression levels were calculated using the $2^{-\Delta\Delta Ct}$ method, with the levels normalized to GAPDH mRNA. Sequences of the real-time PCR primers were: IGF2BP3 (Forward, 5'-TATATCGGAAACCTCAGCGAGA-3'; Reverse, 5'- GGACCGAGTGCTCAACTTCT-3'); METTL14(Forward, 5'-AGTGCCGACAGCATTGGTG-3'; Reverse, 5'- GGAGCAGAGGTATCATAGGAAGC-3'); GADPH(Forward, 5'-ACAGTCAGCCGCATCTTCTT-3'; Reverse, 5'-GACAAGCTTCCCGTTCTCAG-3');

Western blotting

Treated CRC cells were extracted by RIPA lysis buffer and quantified by BCA Protein Assay Reagent Kit (Thermo Fisher Scientific). 20-50 μg of protein was separated by SDS-polyacrylamide gels and then transferred to PVDF membranes (Millipore). The membranes were blocked with 5% nonfat milk for 1-2 hours and incubated with primary antibody at 4℃ overnight. Anti-α-tubulin monoclonal antibody (T6199; Sigma) was used as a loading control. The primary antibodies were IGF2BP3 (Abcam, ab208869, 1:400), EGFR (Abcam, ab52894, 1:1000), ERK (Cell Signaling Technology, #4695S, 1:200), p-ERK (Cell Signaling Technology, #4370S, 1:200), JUK (Cell Signaling Technology, #9251S, 1:200), p-JUK (Cell Signaling Technology, #9255S, 1:200), METTL14 (Solarbio, K107984P, 1:4000). Secondary antibodies (1:8000) were labeled with HRP. The ECL detection system (KeyGEN) was used for visualization.

Histology and immunohistochemistry

Tissue samples were fixed with 4 % paraformaldehyde. After incubation, the samples were washed and dehydrated in graded ethanol. After appropriate permeation in xylene, the fixed tissues were embedded in paraffin and followed by cutting 2.5 μm paraffin sections. Then they were de-paraffinized xylene twice and rehydrated in descending concentration of ethanol. Standard hematoxylin-eosin (HE) staining of paraffin-embedded tissue was used for histological examination.

The sections along the HE stained slides were further processed for immunohistochemistry. The protein expression levels of IGF2BP3, EGFR, and METTL14 were determined by IHC analysis. Briefly, the slides were incubated with primary antibodies: IGF2BP3 (Altas Antibodies, HPA002037, 1:200), EGFR (Abcam, ab52894, 1:1000), METTL14 (Solarbio, K107984P, 1:50), at 4 ℃ overnight. The subsequent steps were

performed using the SP-9000 SPlink Detection Kit (ZSGB-BIO) according to the manufacturer's instructions. The final stainings were scored according to immunoreactivescore (IRS) analysis: staining intensity (SI), 0 (no staining), 1 (weak), 2 (moderate), or 3 (strong); percentage of positive cells (PP), 0 (negative staining), 1 (1%-10% positive staining), 2 (10%-25% positive staining), 3 (25%-50% positive staining), and 4 (50%-75% positive staining). SI and PP were multiplied to give a final score. The tissues with a final score ≤3 were classified as 'Low Expression' and the tissues with a final score >3 were classified as 'High Expression'.

Establishment of Stable IGF2BP3 and EGFR Knockdown and Overexpression cells

The IGF2BP3 and EGFR construct was generated by subcloning PCR amplified full-length human IGF2BP3 and EGFR cDNA into pEZ-Lv105. Stable knockdown of target genes was achieved by lenti-viral based short-hairpin RNA delivery. Target specific shRNAs were cloned into lenti-viral vector pLKO.1. Viral particles were packaged in 293FT and used to infect SW480 and HCT116 cell lines. Infected cells were selected by puromycin and expanded to form a stable sub-line. Knockdown efficiency was confirmed at both mRNA and protein levels. A non-target control shRNA purchased from Sigma-Aldrich was used as a negative control. The target sequence of IGF2BP3 was shRNA1 (Forward, 5'-CCGGCGGTGAATGAACTTCAGAATTCTCGAGAATTCTGAAGTTCATTCACCGTTTTTG - 3'; Reverse, 5'-AATTCAAAAACGGTGAATGAACTTCAGAATTCTCGAGAATTCTGAAGTTCATTCACCG-3'); shRNA2 (Forward, 5'- CCGGGCAGGAATTGACGCTGTATAACTCGAGTTATACAGCGTCAATTCCTGCTTTTTG

-3'; Reverse, 5'-AATTCAAAAAGCAGGAATTGACGCTGTATAACTCGAGTTATACAGCGTCAATTCCTGCTTTTTG -3');

Establishment of IGF2BP3 Knockout Cells

IGF2BP3 knockout in SW480 was generated using CRISPR/Cas9 technology by lentiviral transduction and puromycin selection. Cas9 and single guide RNAs (sgRNAs) lentivirus were bought from Genechem. SW480 cells were first engineered to express Cas9. sgRNAs targeting IGF2BP3 were cloned into the lentiCRISPR vector. SW480 cells were transduced with lentiCRISPR-IGF2BP3 and selected with puromycin. The knockout cell clones were isolated by limited serial dilution. A monoclonal cell line was generated, and the IGF2BP3 knockout effect was confirmed using Western blot and sequencing analysis. The sgRNA sequence targeting IGFBP3 was listed as follows: sg1(Forward, 5'-CTAAACTTCCATGTTGGCTATTATTG-3'; Reverse, 5'-CAATATTTGGTTTCTTATCCCAAAG-3'); sg2(Forward, 5'- GAAATGGCCGCCCAGCAAAACC-3'; Reverse, 5'- CACATTCCCAAGTACTGTACAAG-3'). A non-target control shRNA was used as a negative control.

In vitro cell proliferation, migration, and invasion assays

A colony-forming assay was used to determine the proliferation of cells. Cells were seeded in 6-well culture plates at a concentration of 200 cells per well. The cells were cultured for 14 days and then washed two times with PBS, fixed in 4% (vol/vol) paraformaldehyde, and stained with 0.1% (wt/vol)

crystal violet solution. The colonies were counted under the microscope (1 colony for more than 50 cells). For the MTT assay, 1000 cells were seeded and transfected in a 96-well plate. After 24h, 5 mg/ml MTT solution was added to each well and the cells were incubated with MTT for 4 h in standard conditions. Then, the supernatant was removed. In all wells, 10 μl DMSO for MTT crystals dilution were added. The absorbance was measured at 570 nm using an automated microplate reader. For soft agar assay, each well of a six-well culture dish was coated with 2 ml bottom agar mixture (DMEM or 1640, 1.32% (w/v) agar). After the bottom layer had solidified, 2 ml top agar-medium mixture (DMEM or 1640, 0.66% (w/v) agar) containing 1×10^5 cells were added, and the dishes were incubated at 37°C for 2 weeks. The plates were stained with Crystal Violet, then the number of colonies was counted by a dissecting microscope. Experiments were repeated three times.

Mouse experiments

In vivo experiments were all performed on 4-6-week-old female BABL/cAnN-nude mice bought from Southern Medical University Animal Center. For the subcutaneous implantation model, 2×10^6 cells were first suspended in 200 ul serum-free medium and then were injected subcutaneously in the right flank. After one week, the tumor volumes were measured every day. Mice were sacrificed at week 4 to harvest the tumor bulks. For in vivo cetuximab treatment, one week after subcutaneous implantation, mice were randomized into control (0.9% NaCl), low dose cetuximab (1 mg/kg), and high dose cetuximab (2 mg/kg) groups, intraperitoneal (i.p.) injection, every 3 days. Mice were sacrificed at week 14 to harvest the tumor bulks. Tumor volume was calculated by the formula $V = ab^2/2$, where a and b are the tumor's length and width, respectively.

Luciferase reporter assay

The fragments of EGFR-3'UTR containing the wild-type m^6A motifs as well as mutant m^6A motifs (m^6A was replaced by T) were synthesized at HanYi Biology Technologies. The wild-type and mutant EGFR-3'UTR fragments were inserted into the upstream of pmirGLO-basic firefly luciferase vector. CRC cells were seeded in 24-well plates and transfected with 5ug wild-type or mutant EGFR-3'UTR. The relative luciferase activity was detected using the Dual-Luciferase Reporter Assay System (Promega) 48 hours later. Firefly luciferase activity and Renilla luciferase activity were measured using Synergy NE02 (BioTek). The results were shown in the form of relative firefly luciferase activity normalized to Renilla luciferase activity. All the experiments were repeated three times, and three replicates were conducted for each group.

mRNA stability analysis

Cells with or without IG2BP3 overexpressed and knockouted were directly treated with Actinomycin D for 0h, 3h, and 6h at a final concentration of 5 μg/mLand harvested at the indicated time points. Total RNA was extracted, and real-time PCR was conducted to quantify the relative level of EGFR mRNA. The

degradation rate and half-life of EGFR mRNA were estimated according to the published paper. Briefly, the degradation rate of mRNA (K_{decay}) was calculated by the following equation:

$$\ln(C/C_0) = -K_{dacay}t$$

t is the transcription inhibition time, and C is the mRNA level at the time t. C_0 is the level of mRNA at 0 hour in the equation, which means the mRNA level before decay starts. Thus, the mRNA half-time (t1/2) can be calculated by the equation

$$\ln(1/2) = -K_{decay}t_{1/2}$$

m^{6}A dot blot

Polyadenylated mRNA was purified by GenEluteTM mRNA Miniprep Kit (Sigma) from previously isolated total RNA. The poly(A)+ RNA samples were loaded to Hybond-N+ membrane (GE Healthcare) and UV crosses with the nylon membrane. The membrane was then blocked with 5% nonfat milk for 1 hour and incubated with m^{6}A antibody (Abcam, 190886) at 4°C, overnight. After incubating with horseradish peroxidase-conjugated anti-mouse IgG, the membrane was visualized with the ECL detection system. The relative signal density of each dot was quantified by Image J software. The results of m^{6}A level were shown in the form of relative m^{6}A dot blot density normalized to methylene blue staining density.

MeRIP and MeRIP-qPCR

Total RNA was extracted by Trizol reagent (Takara), and mRNA was purified using GenEluteTM mRNA Miniprep Kit (Sigma). RNA fragmentation reagents (NEB) were used to randomly fragment RNA. The specific anti-m^{6}A antibody (NEB) was applied for m^{6}A immunoprecipitation. Anti-m^{6}A antibody was pre-bound to Protein G magnetic beads in reaction buffer for 30 minutes. The fragmented mRNA was incubated with m^{6}A-antibody-bound protein G magnetic beads at 4°C for 1 hour and washed with low salt reaction buffer and high salt reaction buffer. M^{6}A-antibody-bound RNA was extracted from the Dynabeads using Buffer RLT (Qiagen) and further incubated with Dynabeads MyOne Silane (Life Technologies). The RNA and Dynabeads mixture were precipitated with 100% ethanol washed with 70% ethanol and then re-suspend with nuclease-free water. The supernatant was carefully collected after the beads were pulled to the side of the tube by a magnetic field. Real-time PCR was carried following m^{6}A-IP to quantify the changes to m^{6}A methylation of EGFR. Sequences of the real-time PCR primers of EGFR were: forward, 5'- GATGGGCAGGTCAGGAGA-3'; reverse, 5'- CCAGGCTATCAATCAGGAAG-3').

DAA (3-Deazaadenosine) inhibit experiment

The DAA inhibit experiments were performed as described previously [15]. Cells were seeded in 96-well culture plates. 4ug/ml DAA (APExBIO, B6121) were added. MTT assay were then performed to calculate the inhibition rate.

Statistical analysis

Statistical analyses were carried out using SPSS 20.0. Data are presented as means±SD from three independent experiments. For continuous variables, data were analyzed by two-tailed unpaired Student's t test between two groups and by one-way ANOVA for multiple comparisons. For categorical variables, Chi-square test was used. The overall survival rate curves based on Kaplan-Meier method were plotted using the log-rank test. The correlation between IGF2BP3 expression and EGFR and METTL14 expression was determined by Spearman correlation analysis. P values less than 0.05 were considered statistically significant.

Results

IGF2BP3 is up-regulated in CRC tissues, and is a prognostic biomarker for CRC

We conducted RNA sequencing (RNA-Seq) to compare the gene expression profiles in 11 pairs of primary tumors and their corresponding normal intestinal mucosa and lymph node metastases from CRC patients. We identified that IGF2BP3, an RNA-binding protein, was significantly up-regulated in primary tumor and lymph node metastasis (Fig. 1a). Further analysis of data from GEO (GSE41258, GSE71187), Oncomine (www.oncomine.com), and the cBioPortal for Cancer Genomics databases all suggested that the expression of IGF2BP3 in CRC was higher than that in normal tissues (Fig. 1b, Fig. S1a-c). Western blot and qPCR further confirmed the up-regulation of IGF2BP3 in CRC (Fig. 1c-d, Fig. S1d). Immunohistochemistry staining results also proved that the high expression of IGF2BP3 was significantly correlated with poorer differentiation (Fig. 1e).

In 1983, Pierce DB expressed the idea that carcinogenesis is an epigenetic event, similar to postembryonic differentiation [16]. Previous researches have revealed that IGF2BP3 is expressed in most organs during embryogenesis, but becomes either absent or expressed at very low levels in most tissues after birth [17]. Therefore, we analyzed the expression profile chip of mouse early colon embryonic development (GSE38831). In accord with previous studies, a gradual decrease of IGF2BP3 expression with embryonic development was observed (Fig. S1e). In addition, analysis of GSE71187 showed that the expression of IGF2BP3 in both embryonic and CRC tissues was higher than that of normal intestinal mucosa tissues (Fig. S1b). We found that IGF2BP3 showed a spatiotemporal expression pattern of 'high expression during embryogenesis, inhibited expression in normal intestinal mucosa, and up-regulated expression in CRC tissues', which suggests that IGF2BP3 may be involved in tumorigenesis and tumor progression of CRC.

Moreover, interrogation of GEO dataset (GSE17536 and GSE17537) revealed that a higher level of IGF2BP3 was significantly associated with shorter overall survival in patients with CRC (Fig. 1f-g). Elevated expression of IGF2BP3 was also significantly associated with certain clinicopathological features like TNM staging and Dukes staging (Table S1). Taken together, these results suggest that IGF2BP3 may be a prognostic biomarker for CRC.

IGF2BP3 regulates the stability of EGFR mRNA

As an RNA binding protein, IGF2BP3 can promote the stability and translation by binding to the non-coding region of the target mRNA. To delineate the functional implications of IGF2BP3 and identify its downstream targets in CRC, we established stable IGF2BP3-overexpressing and IGF2BP3-knockdown or knockout CRC cell lines (Fig. S2a-c). Gene ontology and KEGG analysis of IGF2BP3 knockout cells revealed that down-regulated genes were significantly enriched in ERBB Network Pathway gene set (Fig. 2a-b). As one of the ERBB receptors, EGFR has been identified as an oncogene and was the first growth factor receptor to be proposed as a target for cancer therapy [10]. An analysis of the downstream genes of EGFR pathway revealed that the overexpression of IGF2BP3 significantly upregulated the phosphorylated levels of p-ERK and p-JUK (Fig. 2c, Fig. S2d). The data from the cBioPortal for Cancer Genomics databases suggested that the activation of EGFR is mostly induced by mutations, not by amplification (Fig. S2e). Then we used GSE41258 chip to analyze the expression of EGFR, which showed that there was no significant difference in the expression of EGFR mRNA in normal tissues and tumor tissues (Fig. S2f).

IGF2BP3 serves as a posttranscriptional regulatory factor for mRNA [18]. Therefore, we hypothesized that the regulation of EGFR protein by IGF2BP3 may be due to a difference in mRNA stability. The RNA stability curves showed that knockdown of IGF2BP3 reduced the half-life of EGFR mRNA, while overexpression of IGF2BP3 lengthen it (Fig. 2d). Taken together, IGF2BP3 activates the EGFR signaling pathway by maintaining EGFR mRNA stability.

IGF2BP3 stabilizes EGFR mRNA in an m^{6}A-dependent manner.

Besides traditional RBS, previous research has demonstrated that as m^{6}A readers, IGF2BPs bind to m^{6}A RNAs and regulate their stability [3]. Consistently, m^{6}A dot-blot analysis showed an evident relevance between IGF2BP3 and m^{6}A levels (Fig. 3a). In accord with the previous finding that IGF2BP3 preferentially bound to the most common m^{6}A motif ‘GGAC’ [3], we identified GGAC as the m^{6}A consensus motif and presented that the GGAC motif was enriched in 3'UTRs of EGFR mRNA (Fig. S3a-c). To further address the effect of m^{6}A modification on EGFR mRNA gene, we constructed both wild-type and mutant (m^{6}A was replaced by T) EGFR luciferase reporter plasmids (Fig. 3b-c). As expected, knockout of IGF2BP3 substantially reduced luciferase activity of the reporter constructs bearing wild-type EGFR 3’ UTR with intact m^{6}A sites, while overexpression of IGF2BP3 increased it. However, neither knockout nor overexpression of IGF2BP3 had a significant effect on the luciferase activity reporter plasmids with m^{6}A sites mutations in SW480 cells (Fig. 3c). This finding was further supported by the MeRIP assay, which showed that knockout or overexpression of IGF2BP3 downregulated or upregulated, respectively, the m^{6}A levels of EGFR in SW480 cells (Fig. 3d).

Functions of m^{6}A in RNA metabolisms are carried out by its readers, while dynamic transcriptomic m^{6}A modification is orchestrated by its writers and erasers [13]. Fig. S3a shows the proportion of readers, writers, and erasers of m^{6}A regulators [19]. To identify the corresponding m^{6}A writer of EGFR mRNA, we

carried out real-time PCR and Western blot assays. The level of METTL14, an m^6A writer, decreased in IGF2BP3-knockout cells and increased in IGF2BP3-overexpressing cells (Fig. 3e-f), which indicated that METTL14 may be the m^6A writer of EGFR mRNA. Together, these results suggest that IGF2BP3 serves as a reader and increases EGFR expression by stabilizing EGFR mRNA in an m^6A-dependent mechanism partnered by METTL14.

IGF2BP3 induces tumor cell proliferation depending on the expression of EGFR in CRC.

We next verified the effect of IGF2BP3 on CRC proliferation. We observed that overexpression of IGF2BP3 promoted cell proliferation and enhanced colony formation, whereas knockdown of IGF2BP3 significantly suppressed cell proliferation and inhibited colony formation (Fig. 4a-c, Fig. S4a-d). Furthermore, overexpression of IGF2BP3 dramatically increased tumor volumes in xenograft mouse models, while knockdown of IGF2BP3 effectively suppressed tumor growth (Fig. 4d-g).

In addition, we investigated whether EGFR participated in the biological function of IGF2BP3 in CRC. Downregulation of EGFR dramatically impaired IGF2BP3-induced cell proliferation, colony formation, and tumorigenesis, while overexpression of EGFR partially restored the proliferation, colony formation, and tumorigenesis ability of IGF2BP3-knockdown cells (Fig. 4a-g, Fig. S4a-d), which supported EGFR as a critical target gene of IGF2BP3 in CRC. Taken together, our results suggest that IGF2BP3 may promote tumor cell proliferation via activation of the EGFR signaling pathway.

IGF2BP3 affects the sensitivity of CRC cells to cetuximab.

The EGFR-directed monoclonal antibodies cetuximab is now widely used in combination with chemotherapy or as monotherapy for CRC (Fig. 5a). However, resistance to cetuximab inevitably occurs, thereby limiting the clinical benefit of this drug. Analyzation of GSE56386 microarray revealed that the expression of IGF2BP3 was significantly higher in patients who did not respond to cetuximab than in those who responded (Fig. S5a). Therefore, we hypothesized that high expression of IGF2BP3 may reduce drug response and induce drug resistance of CRC cells to cetuximab. To test the hypothesis, we selected KRAS, PIK3CA, and BRAF-unmutated Caco2 cells for follow-up experiments. Western blot showed that the addition of cetuximab to Caco2 cells in the control group significantly reduced the protein levels of EGFR and its downstream effector molecules, while the effect of the same dose was less evident in IGF2BP3 overexpressing cells. In contrast, compared with the control group, after interference with IGF2BP3, it only required a lower dose of cetuximab to cause significant down-regulation of the expression of EGFR and its downstream target genes (Fig. S5b, Fig. 5b). In addition, we observed that cetuximab significantly suppressed cell proliferation and colony-formation abilities, while the effect of the same dose was impaired in IGF2BP3 overexpressing cells and enhanced in IGF2BP3 knockdown cells (Fig. 5d-d, Fig. S5c-d). The result was further verified in xenograft mouse models, in which the ability of cetuximab to reduce the tumor growth rate and volume were hindered by overexpression of IGF2BP3 and promoted by downregulation of IGF2BP3 (Fig. 5e-f). These data indicate that high expression of IGF2BP3 increases drug resistance of CRC cells to cetuximab.

The level of IGF2BP3 is clinically relevant in CRC patients.

We next performed immunohistochemical staining on CRC tissue. Samples with high IGF2BP3 expression displayed strong staining for EGFR and METTL14. In contrast, samples with low expression of IGF2BP3 appeared low levels of EGFR and METTL14 (Fig. 6a-b).

So far, we have proved that IGF2BP3 maintains the stability of EGFR mRNA levels by combining METTL14 in an m^6A-dependent manner, and causes drug resistance of CRC cells to cetuximab. We next hypothesized that CRC patients with higher IGF2BP3 expression are more sensitive to anti-tumor drug candidates targeting IGF2BP3. To test this prediction, we treated RKO cells which express a lower IGF2BP3 level with DAA (3-Deazaadenosine), an inhibitor of the internal N6-Methyladenosine [20]. DAA treatment resulted in only 25% inhibition of cell proliferation in RKO cells. Conversely, treatment in SW480, which has a higher expression of IGF2BP3, with the same dose of DAA, resulted in 54% inhibition rate (Fig. 6C). These inhibition results were similar in vivo. DAA is more efficient to inhibit tumor weight in mice bearing SW480 cells than those bearing RKO cells (Fig. 6D). Taken together, these data suggest that targeting m^6A may be more effective in CRC cells with higher IGF2BP3 expression than in those with lower IGF2BP3 expression.

Discussion

CRC accounts for approximately 10% of all annually diagnosed cancers and cancer-related deaths worldwide. Although genetic studies of CRC have identified a number of alterations in crucial genes [21], it is still essential to explore additional genetic and epigenetic factors that contribute to the initiation and development of CRC so as to identify novel therapeutic targets or biomarkers. In the current study, we confirmed the upregulation of IGF2BP3 in CRC samples and revealed that the high expression of IGF2BP3 is negatively correlated with clinical prognosis. We further provided evidence that overexpression of IGF2BP3 enhanced CRC tumorigenesis and progression in vitro and in vivo, and identified EGFR as an important IGF2BP3 target gene. Mechanistically, IGF2BP3 promoted EGFR expression and activated its downstream signaling by stabilizing EGFR mRNA through an m^6A-dependent manner. We also demonstrated that high expression of IGF2BP3 increases drug resistance of CRC cells to the EGFR-targeted antibody cetuximab.

RNA-binding proteins (RBPs) play a major role in RNA network control as regulators of the RNA life cycle from alternative splicing to nuclear export, transcript storage, stabilization, localization, and degradation [22]. Alterations in RBP expression may result in aberrant RNA translation and lead to the emergence and progression of several pathological conditions, including cancer. Among the RBPs, IGF2BP3 is of particular interest in tumorigenesis and tumor progression. IGF2BP3 was named because it was originally identified as a posttranscriptional regulator of the fetal growth factor IGF2 [23]. It is expressed during embryogenesis while absent in adult tissues and has been explicated to be upregulated and play a potential oncogenic role in various tumor types. Although previous studies showed that IGF2BP3 promoted the aggressive phenotypes of CRC cells [24] and regulates cell cycle and angiogenesis

in colon cancer [25], the molecular mechanisms of IGF2BP3 in CRC progression and drug resistance remain largely unclear. In the present study, we revealed that the IGF2BP3 level was significantly upregulated in CRC tissues. Furthermore, the high IGF2BP3 expression leads to worse overall survival in CRC patients. These aforementioned findings indicate the potential value of IGF2BP3 as a biomarker for the prediction of CRC and a favorable survival outcome prognostic factor consistent with the previous studies [8, 9].

A number of IGF2BP3 target genes have been identified including HK2 [26], MYC, and CDK6 [27]. Previous studies suggest that the major mechanism for IGF2BP3 as an oncogene is to stabilize its target genes, consequently promoting proliferation and metastasis of cancer cells. IGF2BP3 can sustain the translation of its target gene mRNA by interacting with other RNA binding proteins [28] or non-coding RNA such as lncRNA [29] and circRNA [26], or by protecting it from miRNA-mediated decay [30]. In this study, we identified EGFR as a target gene of IGF2BP3. IGF2BP3 increased EGFR expression by stabilizing its mRNA. Overexpression of IGF2BP3 facilitated the malignancy of CRC cells in vivo and in vitro. Furthermore, inhibition of EGFR could attenuate the proliferation and progression phenotypes of IGF2BP3-overexpressed CRC cells. Immunohistochemical staining on CRC patients' tissues further confirmed the positive correlation between IGF2BP3 and EGFR. Interestingly, previous studies have proved that EGFR signaling induces IGF2BP3 expression in MDA-MB-468 cells [31] and YD-10B cells [32]. Therefore, a positive feedback loop may exist between the EGFR/MEK/MAPK pathway and IGF2BP3 expression in cancer cells. Moreover, further investigations that whether other genes play important roles in IGF2BP3-mediated cell malignancy via an m^6A-dependent or -independent manner will enhance our understanding of IGF2BP3- associated regulatory network.

M^6A is the most abundant internal modification in mRNAs of eukaryotic cells [33], and regulates almost every aspect of mRNA metabolism, from expression and pre-mRNA processing in the nucleus to translation and mRNA decay in the cytoplasm [34]. Studies have shown that aberrancies in m^6A are associated with a variety of diseases including cancers [35]. M^6A writers, erasers, and readers are proteins that can respectively install, remove, or recognize m^6A motif on mRNAs. They have been considered to be essential for tumorigenesis and tumor progression. As readers, IGF2BPs tend to identify target genes with m^6A modifications and regulate their expression by promoting mRNA stability [3]. Similarly, the results presented here demonstrated that overexpression of IGF2BP3 substantially lengthened the half-life of EGFR mRNA. By m^6A dot-blot, luciferase reporter assay, and MeRIP assay, we confirmed that besides traditional RNA binding site, IGF2BP3 also bound to m^6A on EGFR mRNA to regulate its stability. Through a combination of previous research and bioinformatics analysis, we revealed that IGF2BP3 preferentially bound to the m^6A core motif GGAC. M^6A is installed by a multicomponent methyltransferase complex consisting of Methyltransferase Like 3 (METTL3), METTL14, Wilms Tumor 1 Associated Protein (WTAP), etc [34]. Our data identified METTL14 as one possible corresponding m^6A writer. However, this finding is opposite to several reports about the decreased expression and tumor suppressing function of METTL14 in CRC [36, 37], for METTL14-mediated m^6A modified mRNAs are selectively recognized and bound by YTHDF2, thereby promoting the degradation of

these mRNAs [38]. The reasonable explanations for the contradictory phenomena could be ascribed to the different mRNA regions that m^6A is distributed on and the different reader proteins responding to these m^6A modifications. A previous study has shown that RBM15-mediated m^6A modification of TMBIM6 mRNA enhanced its stability through IGF2BP3-dependent pathway [39], which suggests that besides METTL14, there may be other corresponding m^6A writers warranting further research.

The development of targeted therapies has provided new options for the personalized management of patients with advanced solid tumors. mAbs directed against the EGFR, such as cetuximab and panitumumab, have emerged as important therapeutic agents in the treatment of metastatic CRC patients with all-RAS wild-type tumors. Nevertheless, after a few months of anti-EGFR monoclonal antibody treatment, almost all tumor patients developed drug resistance. Studies have shown that it may be related to secondary mutations of key molecules in the EGFR pathway, especially secondary mutations of KRAS [40]. However, some patients without secondary mutations in the KRAS gene also develop resistance to anti-EGFR monoclonal antibody therapy, and the specific molecular mechanism is not yet clear. In our study, we presented the first study that IGF2BP3 is associated with drug resistance of EGFR-targeted antibodies cetuximab in CRC cells. IGF2BP3 can stabilize EGFR mRNA through m^6A modification when KRAS is wild-type, thereby continuously activating the downstream signaling pathway of EGFR, promoting the tumorigenesis and evolution of CRC, and then affecting the sensitivity of CRC patients to anti-EGFR monoclonal drug therapy. This finding is consistent with previous studies identifying drugs and miRNAs that down-regulate EGFR expression in cancer cells and potentiate the effects of cetuximab [41, 42]. Our studies have implied a critical role for IGF2BP3 in predicting the prognosis of cetuximab treatment.

In short, IGF2BP3 plays an oncogenic role in stabilizing EGFR mRNA via an m^6A-dependent manner and further regulates cancer cell proliferation and drug resistance to cetuximab in CRC cells (Fig. 6E). In addition to IGF2BP3 biological and epigenetic importance, our work may be relevant to the clinical management of CRC patients, as IGF2BP3 may be promising biomarkers to guide early diagnosis and therapy in CRC. We further found that DAA, a chemical inhibitor of the internal N6-Methyladenosine, is more effective to inhibit cell proliferation in CRC cells with higher IGF2BP3 expression than those cells with lower IGF2BP3 expression. Since DAA also inhibits other signal pathways [43, 44], a more specific inhibitor of IGF2BP3 needs to be developed for CRC patients. Therefore, the combined treatment with anti-EGFR drugs, such as cetuximab, and with specific inhibitor for IGF2BP3 or m^6A, could be a potential therapeutic strategy to investigate in a clinical setting for overcoming intrinsic or acquired resistance to EGFR inhibitors in CRC patients.

Conclusion

In summary, we elucidated the critical role of IGF2BP3 in CRC as a functional and clinical oncogene, wherein it stabilizes EGFR mRNA via an m6A-dependent manner and further promotes CRC progression and drug resistance to cetuximab. These findings shed light on novel molecular mechanisms of CRC

tumorigenesis and progression. Combining IGF2BP3 or m6A-specific inhibitors with anti-EGFR drugs (such as cetuximab) may provide an effective treatment strategy for CRC patients who are resistant to EGFR inhibitors.

Abbreviations

IGF2BP3: Insulin-like growth factor 2 mRNA-binding protein 3; CRC: CRC; m^6A: N6-methyladenosine; EGFR: epidermal growth factor receptor; RNA-binding protein: RBP; GEO: Gene expression omnibus; HE: Hematoxylin and eosin; IHC: Immunohistochemistry; qRT-PCR: Quantitative RT-PCR; shRNA: short hairpin RNA; siRNA: small interfering RNA; TCGA: The Cancer Genome Atlas; METTL14: Methyltransferase-like 14; MeRIP: Methylated RNA immunoprecipitation; DAA: 3-Deazaadenosine

Declarations

Acknowledgements

We thank the Central Laboratory of Southern Medical University for technical supports.

Authors contributions

JHL, YYP and DYQ designed the experiments; JHL, YYP, CLJ, and XZY analyzed the data, wrote the manuscript, and directed the research. WSY, QT, ZD and ZLJ performed experiments. HFY, CGJ conducted vector construction. XXM and ZJH provided research materials and methods. All authors read and approved the final manuscript.

Funding

This work was supported by the National Natural Science Foundation of China (81972756, 82173185, 81874194, 82072713, 81902476, 81773101, 81972754, 81773196, 82073236, 82103256).

Availability of data and materials

The high-throughput RNA sequencing data have been deposited National Natural Science Foundation of China (Grant No. U1201226). All the other data supporting the findings of this study are available within the article and its Supplementary Information files and from the corresponding author upon reasonable request.

Ethics approval and consent to participate

The research was approved by the Ethics Committee of Nanfang Hospital, Southern Medical University (Guangzhou, China). This study was carried out in strict accordance with the recommendations in the Guide for the Care and Use of Laboratory Animals of the National Institutes of Health. The protocol was approved by the Committee on the Ethics of Animal Experiments of Southern Medical University.

Consent for publication

All of the patients provided signed, informed consent before the use of these clinical materials for research purposes.

Competing interests

The authors declare that they have no competing interests.

Author details

[1] Department of Pathology, Nanfang Hospital, Southern Medical University, Guangzhou, Guangdong, China. [2] Department of Pathology, School of Basic Medical Sciences, Southern Medical University, Guangzhou, Guangdong, China. [3]Guangdong Provincial Key Laboratory of Molecular Tumor Pathology, Guangzhou, Guangdong, China. [4] Department of Pathology, Shenzhen People's Hospital, Second Clinical Medical College of Jinan University, Shenzhen, Guangdong, China.

References

1. Cardoso R, Guo F, Heisser T, Hackl M, Ihle P, De Schutter H, Van Damme N, Valerianova Z, Atanasov T, Májek O *et al*: **Colorectal cancer incidence, mortality, and stage distribution in European countries in the colorectal cancer screening era: an international population-based study**. *Lancet Oncol* 2021, **22**(7):1002-1013.
2. Akimoto N, Ugai T, Zhong R, Hamada T, Fujiyoshi K, Giannakis M, Wu K, Cao Y, Ng K, Ogino S: **Rising incidence of early-onset colorectal cancer - a call to action**. *Nat Rev Clin Oncol* 2021, **18**(4):230-243.
3. Huang H, Weng H, Sun W, Qin X, Shi H, Wu H, Zhao BS, Mesquita A, Liu C, Yuan CL *et al*: **Recognition of RNA N(6)-methyladenosine by IGF2BP proteins enhances mRNA stability and translation**. *Nat Cell Biol* 2018, **20**(3):285-295.
4. Mancarella C, Scotlandi K: **IGF2BP3 From Physiology to Cancer: Novel Discoveries, Unsolved Issues, and Future Perspectives**. *Front Cell Dev Biol* 2019, **7**:363.
5. Huang W, Li Y, Zhang C, Zha H, Zhou X, Fu B, Guo J, Wang G: **IGF2BP3 facilitates cell proliferation and tumorigenesis via modulation of JAK/STAT signalling pathway in human bladder cancer**. *J Cell Mol Med* 2020, **24**(23):13949-13960.
6. Xueqing H, Jun Z, Yueqiang J, Xin L, Liya H, Yuanyuan F, Yuting Z, Hao Z, Hua W, Jian L *et al*: **IGF2BP3 May Contributes to Lung Tumorigenesis by Regulating the Alternative Splicing of PKM**. *Front Bioeng Biotechnol* 2020, **8**:679.
7. Zhou Y, Huang T, Siu HL, Wong CC, Dong Y, Wu F, Zhang B, Wu WKK, Cheng ASL, Yu J *et al*: **IGF2BP3 functions as a potential oncogene and is a crucial target of miR-34a in gastric carcinogenesis**. *Mol Cancer* 2017, **16**(1):77.

8. Li D, Yan D, Tang H, Zhou C, Fan J, Li S, Wang X, Xia J, Huang F, Qiu G *et al*: **IMP3 is a novel prognostic marker that correlates with colon cancer progression and pathogenesis**. *Ann Surg Oncol* 2009, **16**(12):3499-3506.
9. Huang X, Wei Q, Liu J, Niu H, Xiao G, Liu L: **Analysis of IMP3 expression in primary tumor and stromal cells in patients with colorectal cancer**. *Oncol Lett* 2017, **14**(6):7304-7310.
10. Ciardiello F, Tortora G: **EGFR antagonists in cancer treatment**. *N Engl J Med* 2008, **358**(11):1160-1174.
11. Misale S, Di Nicolantonio F, Sartore-Bianchi A, Siena S, Bardelli A: **Resistance to anti-EGFR therapy in colorectal cancer: from heterogeneity to convergent evolution**. *Cancer Discov* 2014, **4**(11):1269-1280.
12. He L, Li H, Wu A, Peng Y, Shu G, Yin G: **Functions of N6-methyladenosine and its role in cancer**. *Mol Cancer* 2019, **18**(1):176.
13. Yang Y, Hsu PJ, Chen YS, Yang YG: **Dynamic transcriptomic m(6)A decoration: writers, erasers, readers and functions in RNA metabolism**. *Cell Res* 2018, **28**(6):616-624.
14. Blanco S, Frye M: **Role of RNA methyltransferases in tissue renewal and pathology**. *Curr Opin Cell Biol* 2014, **31**:1-7.
15. Shen C, Xuan B, Yan T, Ma Y, Xu P, Tian X, Zhang X, Cao Y, Ma D, Zhu X *et al*: **m6A-dependent glycolysis enhances colorectal cancer progression**. *Mol Cancer* 2020, **19**(1):72.
16. Pierce GB: **The cancer cell and its control by the embryo. Rous-Whipple Award lecture**. *Am J Pathol* 1983, **113**(1):117-124.
17. Degrauwe N, Suvà M-L, Janiszewska M, Riggi N, Stamenkovic I: **IMPs: an RNA-binding protein family that provides a link between stem cell maintenance in normal development and cancer**. *Genes Dev* 2016, **30**(22):2459-2474.
18. Cao J, Mu Q, Huang H: **The Roles of Insulin-Like Growth Factor 2 mRNA-Binding Protein 2 in Cancer and Cancer Stem Cells**. *Stem Cells Int* 2018, **2018**:4217259.
19. Li Y, Xiao J, Bai J, Tian Y, Qu Y, Chen X, Wang Q, Li X, Zhang Y, Xu J: **Molecular characterization and clinical relevance of m(6)A regulators across 33 cancer types**. *Molecular cancer* 2019, **18**(1):137.
20. Fustin J-M, Doi M, Yamaguchi Y, Hida H, Nishimura S, Yoshida M, Isagawa T, Morioka MS, Kakeya H, Manabe I *et al*: **RNA-methylation-dependent RNA processing controls the speed of the circadian clock**. *Cell* 2013, **155**(4):793-806.
21. Yaeger R, Chatila WK, Lipsyc MD, Hechtman JF, Cercek A, Sanchez-Vega F, Jayakumaran G, Middha S, Zehir A, Donoghue MTA *et al*: **Clinical Sequencing Defines the Genomic Landscape of Metastatic Colorectal Cancer**. *Cancer Cell* 2018, **33**(1).
22. Qin H, Ni H, Liu Y, Yuan Y, Xi T, Li X, Zheng L: **RNA-binding proteins in tumor progression**. *J Hematol Oncol* 2020, **13**(1):90.
23. Nielsen J, Christiansen J, Lykke-Andersen J, Johnsen AH, Wewer UM, Nielsen FC: **A family of insulin-like growth factor II mRNA-binding proteins represses translation in late development**. *Mol Cell Biol* 1999, **19**(2):1262-1270.

24. Xu W, Sheng Y, Guo Y, Huang Z, Huang Y, Wen D, Liu C-Y, Cui L, Yang Y, Du P: **Increased IGF2BP3 expression promotes the aggressive phenotypes of colorectal cancer cells in vitro and vivo**. *J Cell Physiol* 2019, **234**(10):18466-18479.
25. Yang Z, Wang T, Wu D, Min Z, Tan J, Yu B: **RNA N6-methyladenosine reader IGF2BP3 regulates cell cycle and angiogenesis in colon cancer**. *J Exp Clin Cancer Res* 2020, **39**(1):203.
26. Zhang Y, Zhao L, Yang S, Cen Y, Zhu T, Wang L, Xia L, Liu Y, Zou J, Xu J *et al*: **CircCDKN2B-AS1 interacts with IMP3 to stabilize hexokinase 2 mRNA and facilitate cervical squamous cell carcinoma aerobic glycolysis progression**. *J Exp Clin Cancer Res* 2020, **39**(1):281.
27. Palanichamy JK, Tran TM, Howard JM, Contreras JR, Fernando TR, Sterne-Weiler T, Katzman S, Toloue M, Yan W, Basso G *et al*: **RNA-binding protein IGF2BP3 targeting of oncogenic transcripts promotes hematopoietic progenitor proliferation**. *J Clin Invest* 2016, **126**(4):1495-1511.
28. Li K, Huang F, Li Y, Li D, Lin H, Ni R, Zhang Q, Zhao M, Huang S, Zou L *et al*: **Stabilization of oncogenic transcripts by the IGF2BP3/ELAVL1 complex promotes tumorigenicity in colorectal cancer**. *Am J Cancer Res* 2020, **10**(8):2480-2494.
29. Gu Y, Niu S, Wang Y, Duan L, Pan Y, Tong Z, Zhang X, Yang Z, Peng B, Wang X *et al*: **DMDRMR-Mediated Regulation of m 6 A-Modified CDK4 by m 6 A Reader IGF2BP3 Drives ccRCC Progression** *Cancer Res* 2021, **81**(4):923-934.
30. Wang Z, Tong D, Han C, Zhao Z, Wang X, Jiang T, Li Q, Liu S, Chen L, Chen Y *et al*: **Blockade of miR-3614 maturation by IGF2BP3 increases TRIM25 expression and promotes breast cancer cell proliferation**. *EBioMedicine* 2019, **41**:357-369.
31. Samanta S, Sharma VM, Khan A, Mercurio AM: **Regulation of IMP3 by EGFR signaling and repression by ERβ: implications for triple-negative breast cancer**. *Oncogene* 2012, **31**(44):4689-4697.
32. Hwang YS, Park K-K, Cha IH, Kim J, Chung W-Y: **Role of insulin-like growth factor-II mRNA-binding protein-3 in invadopodia formation and the growth of oral squamous cell carcinoma in athymic nude mice**. *Head Neck* 2012, **34**(9):1329-1339.
33. Roundtree IA, Evans ME, Pan T, He C: **Dynamic RNA Modifications in Gene Expression Regulation**. *Cell* 2017, **169**(7):1187-1200.
34. Yang Y, Hsu PJ, Chen Y-S, Yang Y-G: **Dynamic transcriptomic mA decoration: writers, erasers, readers and functions in RNA metabolism**. *Cell research* 2018, **28**(6):616-624.
35. Wang S, Chai P, Jia R, Jia R: **Novel insights on mA RNA methylation in tumorigenesis: a double-edged sword**. *Mol Cancer* 2018, **17**(1):101.
36. Chen X, Xu M, Xu X, Zeng K, Liu X, Pan B, Li C, Sun L, Qin J, Xu T *et al*: **METTL14-mediated N6-methyladenosine modification of SOX4 mRNA inhibits tumor metastasis in colorectal cancer**. *Mol Cancer* 2020, **19**(1):106.
37. Yang X, Zhang S, He C, Xue P, Zhang L, He Z, Zang L, Feng B, Sun J, Zheng M: **METTL14 suppresses proliferation and metastasis of colorectal cancer by down-regulating oncogenic long non-coding RNA XIST**. *Mol Cancer* 2020, **19**(1):46.

38. Fang Z, Hu Y, Hu J, Huang Y, Zheng S, Guo C: **The crucial roles of N-methyladenosine (mA) modification in the carcinogenesis and progression of colorectal cancer**. *Cell Biosci* 2021, **11**(1):72.
39. Wang X, Tian L, Li Y, Wang J, Yan B, Yang L, Li Q, Zhao R, Liu M, Wang P *et al*: **RBM15 facilitates laryngeal squamous cell carcinoma progression by regulating TMBIM6 stability through IGF2BP3 dependent**. *J Exp Clin Cancer Res* 2021, **40**(1):80.
40. Karapetis CS, Khambata-Ford S, Jonker DJ, O'Callaghan CJ, Tu D, Tebbutt NC, Simes RJ, Chalchal H, Shapiro JD, Robitaille S *et al*: **K-ras mutations and benefit from cetuximab in advanced colorectal cancer**. *N Engl J Med* 2008, **359**(17):1757-1765.
41. Gong J-h, Liu X-j, Li Y, Zhen Y-s: **Pingyangmycin downregulates the expression of EGFR and enhances the effects of cetuximab on esophageal cancer cells and the xenograft in athymic mice**. *Cancer Chemother Pharmacol* 2012, **69**(5):1323-1332.
42. Xing Y, Jing H, Zhang Y, Suo J, Qian M: **MicroRNA-141-3p affected proliferation, chemosensitivity, migration and invasion of colorectal cancer cells by targeting EGFR**. *Int J Biochem Cell Biol* 2020, **118**:105643.
43. Yang WS, Kim JH, Jeong D, Hong YH, Park SH, Yang Y, Jang Y-J, Kim J-H, Cho JY: **3-Deazaadenosine, an S-adenosylhomocysteine hydrolase inhibitor, attenuates lipopolysaccharide-induced inflammatory responses via inhibition of AP-1 and NF-κB signaling**. *Biochem Pharmacol* 2020, **182**:114264.
44. Arumugam MK, Chava S, Rasineni K, Paal MC, Donohue TM, Osna NA, Kharbanda KK: **Elevated S-adenosylhomocysteine induces adipocyte dysfunction to promote alcohol-associated liver steatosis**. *Sci Rep* 2021, **11**(1):14693.

Figures

Figure 1

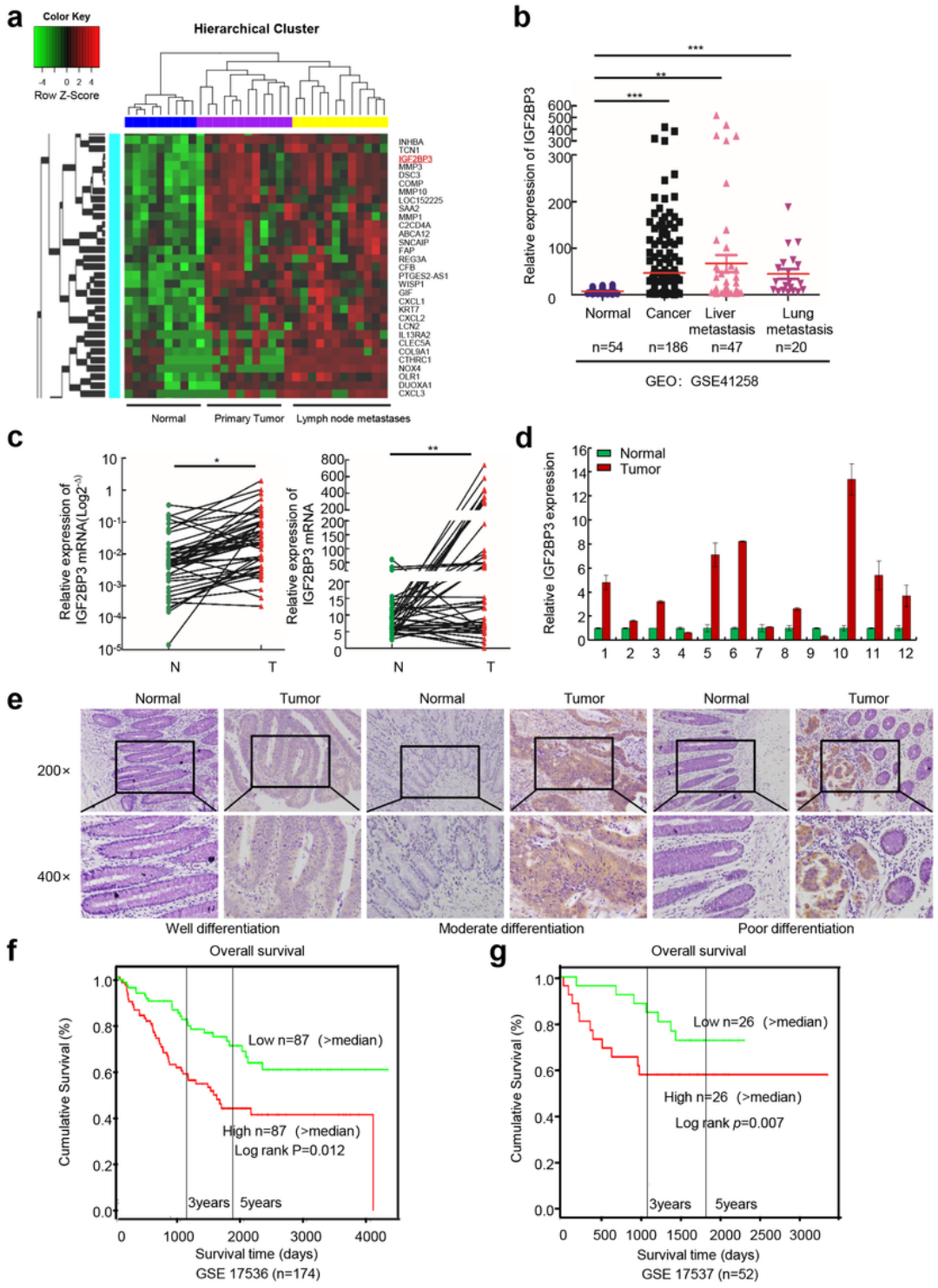

Figure 1

IGF2BP3 is up-regulated in CRC. **a** Different expressed genes in 11 pairs of CRC patients with normal intestinal mucosa, primary tumor, and lymph node metastasis tissues. **b** Expression of IGF2BP3 in normal tissue, CRC, liver metastasis, and lung metastasis from GSE41258 dataset. c Left: relative expression of IGF2BP3 mRNA in 47 cases of fresh CRC paired normal intestinal tissues. Right: relative expression of IGF2BP3 mRNA in CRC tissues and matched normal tissues in TCGA Database. **d**

Quantitation of protein expression of IGF2BP3 in 12 cases of fresh CRC tissues by Western blot. **e** Representative IHC images of IGF2BP3 in well, moderate, and poor-differentiated CRC tissues. **f-g** Kaplan–Meier survival curves of CRC patients with high or low IGF2BP3 expression from GSE17536 (F) and GSE17537 (G) dataset. * p < 0.05; ** p < 0.01; *** p < 0.001;

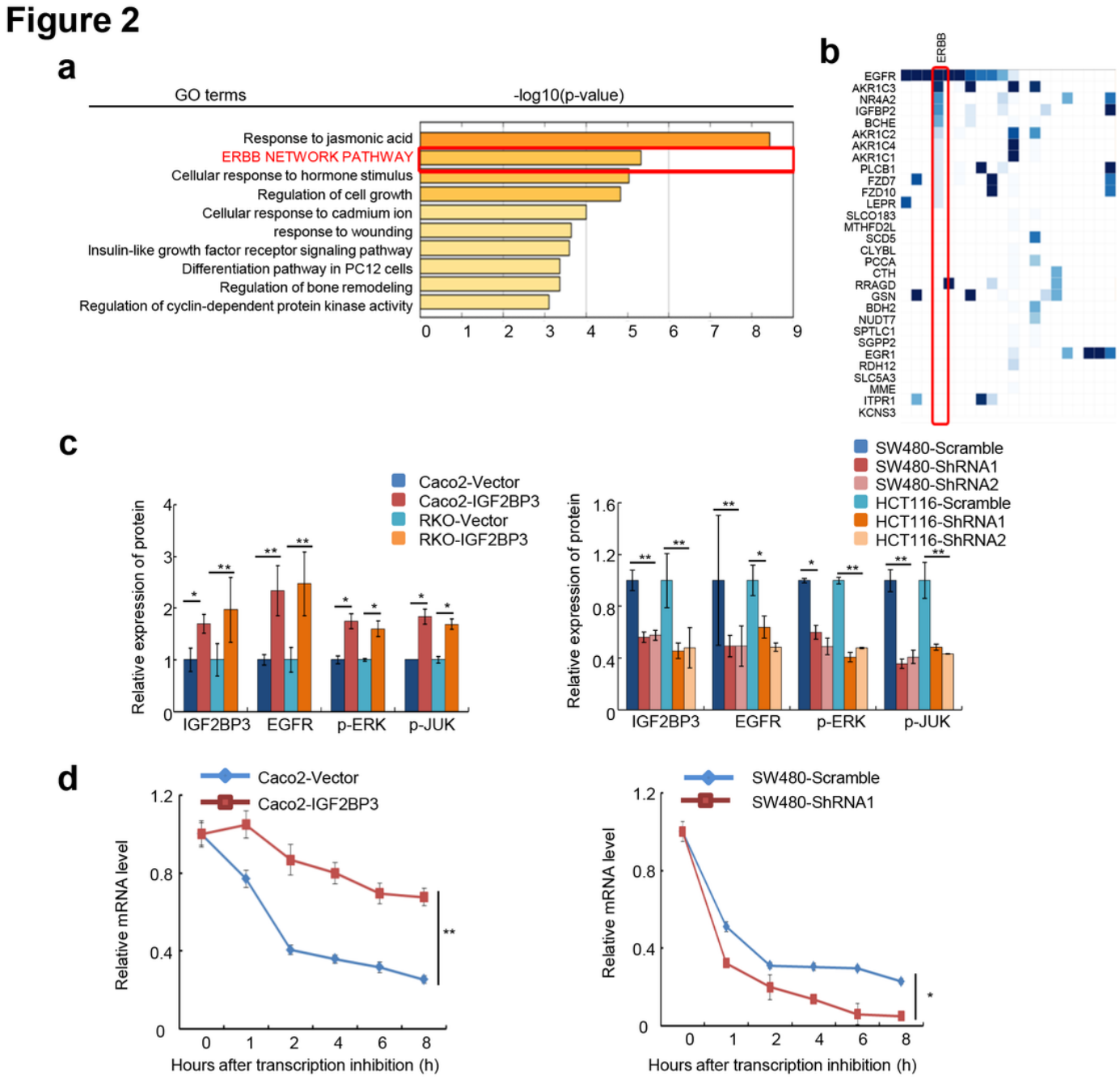

Figure 2

IGF2BP3 regulates the stability of EGFR mRNA. **a** KEGG and GO enrichment. **b** Heat maps of key genes in each pathway. **c** The relative protein expressions of IGF2BP3, EGFR, p-ERK, p-JUK were measured by

Western Blot in Caco2, RKO, SW480, and HCT116 cells after overexpression or knockdown of IGF2BP3, n = 3, nonparametric Mann Whitney test. **d** The EGFR mRNA half-life ($t_{1/2}$) was detected by real-time PCR in Caco2 cells transfected with vector or IGF2BP3 (up) and SW480 cells transfected with scramble or IGF2BP3-ShRNA1 (down). n = 3, nonparametric Mann–Whitney test. * p < 0.05; ** p < 0.01; *** p < 0.001;

Figure 3

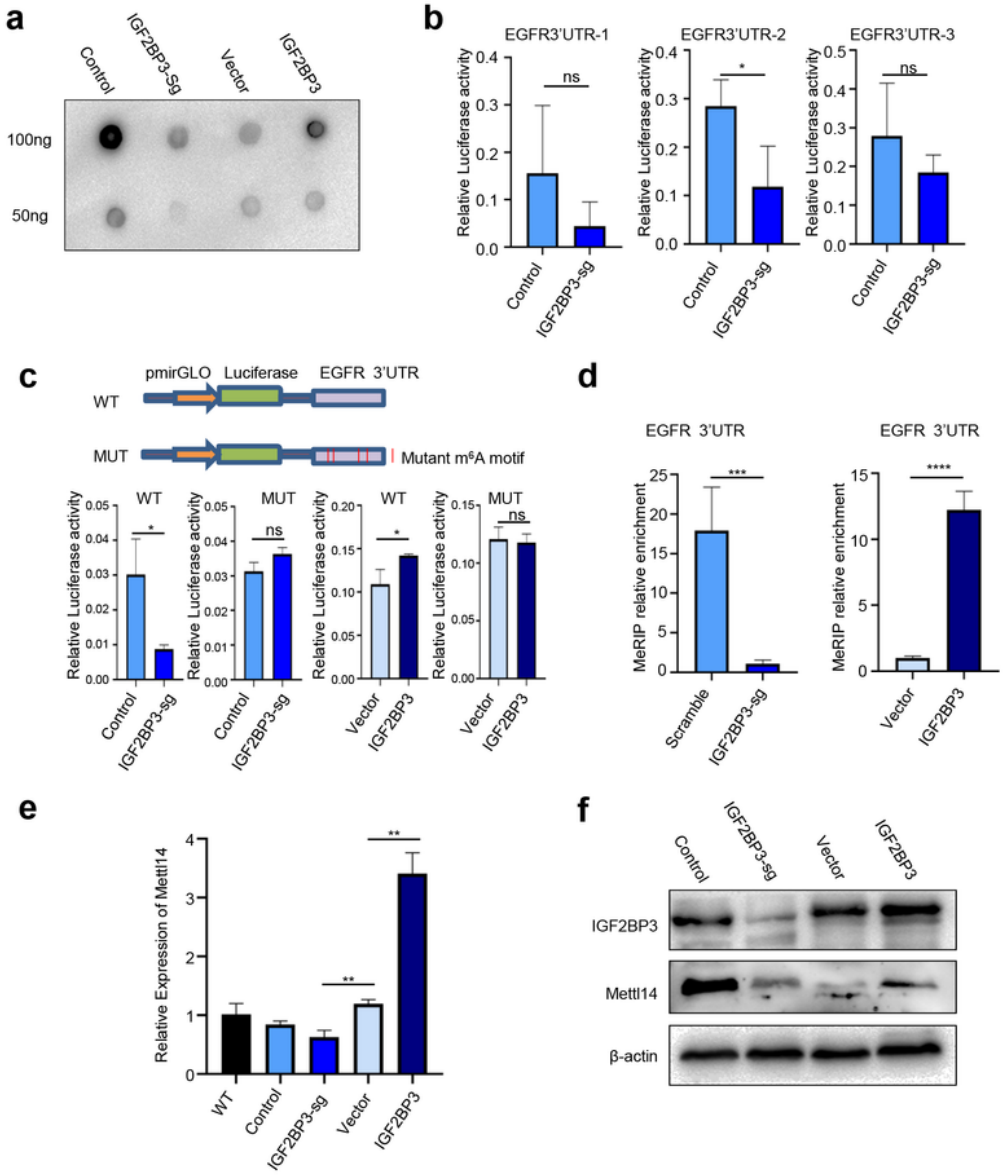

Figure 3

IGF2BP3 stabilizes EGFR mRNA in an m6A-dependent manner. **a** The m^6A dot blot assay of global m^6A abundance in mRNA of SW480 IGF2BP3-overexpressed and IGF2BP3-knockout cells. **b-c** Luciferase activity was measured in SW480 IGF2BP3-knockout cells and SW480 IGF2BP3-control cells transfected with the dual-luciferase reporter plasmids specifically targeting the three predicted m^6A binding sites in the 3'UTR region of EGFR mRNA (**b**) and the luciferase reporters expressing WT or mutant human EGFR 3'UTRs (**c**). **d** MeRIP-qPCR analysis of EGFR 3'UTR m^6A levels in SW480 IGF2BP3-overexpressed and IGF2BP3-knockout cells, n = 3, nonparametric Mann–Whitney test. **e-f** Real-time PCR (**e**) and Western blot assays were performed to analyze the relative Mettl14 levels in SW480 IGF2BP3-overexpressed and IGF2BP3-knockout cells(**f**).

sg, IGF2BP3-knockout. ns, no significance; * $p < 0.05$; ** $p < 0.01$; *** $p < 0.001$; ****$p < 0.0001$;

Figure 4

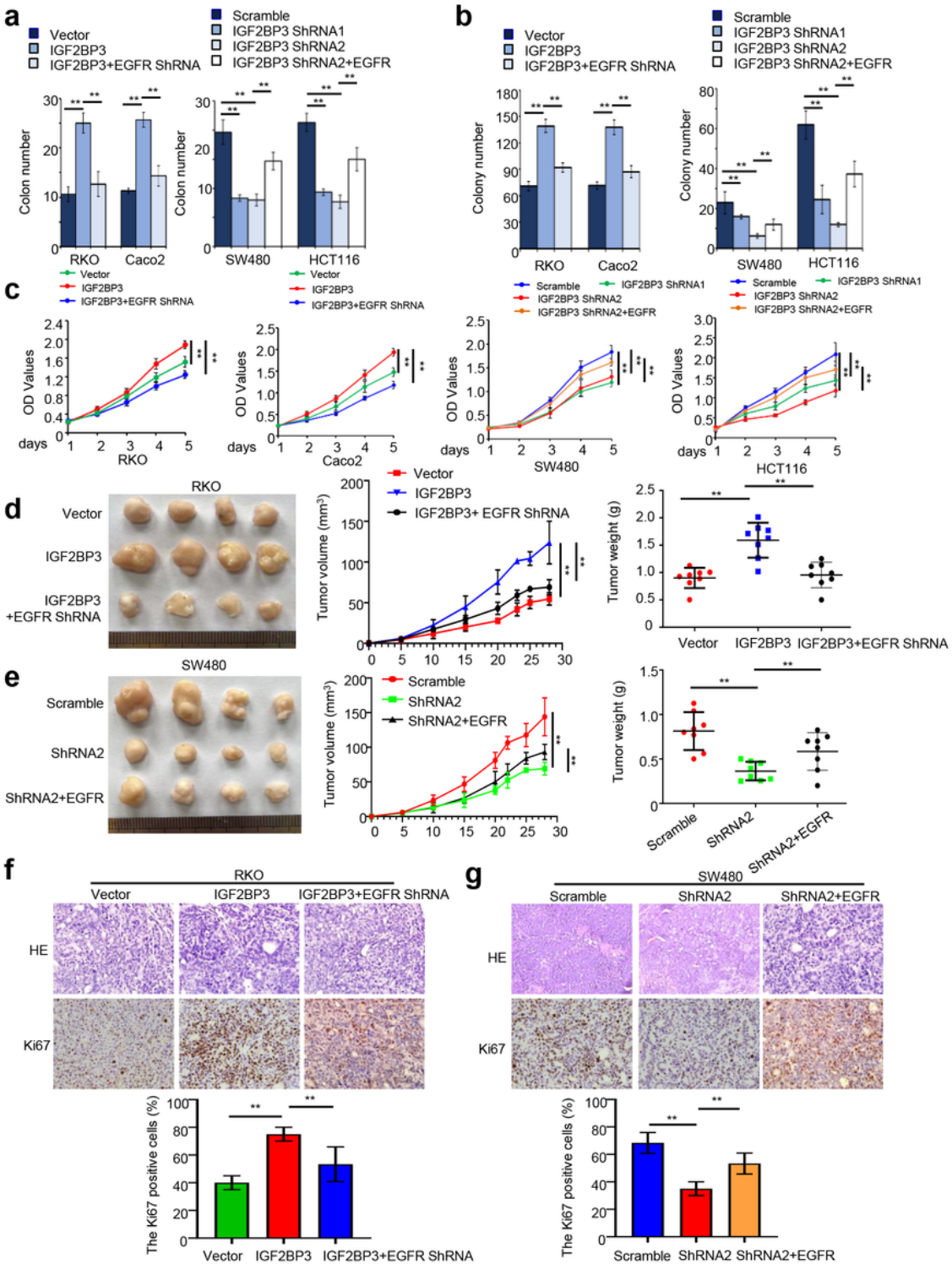

Figure 4

IGF2BP3 induces tumor cell proliferation and tumorigenesis depending on the expression of EGFR in CRC. **a-c** The ability of proliferation of CRC cells were evaluated by the colony formation assay (**a**), soft agar assay (**b**), and MTT assay (**c**) in the indicated cells with different treatments. **d-e** Representative gross images (left), tumor growth rate (middle), and tumor volume analysis (left) of subcutaneous tumors from the indicated groups. n = 8. **f-g** Representative HE staining and IHC images of Ki67 (up), and

the percentage of Ki67 positive cells was quantitatively analyzed (down) in the indicated groups. Error bars represent the mean ± SD of 3 independent experiments; ** p < 0.01.

Figure 5

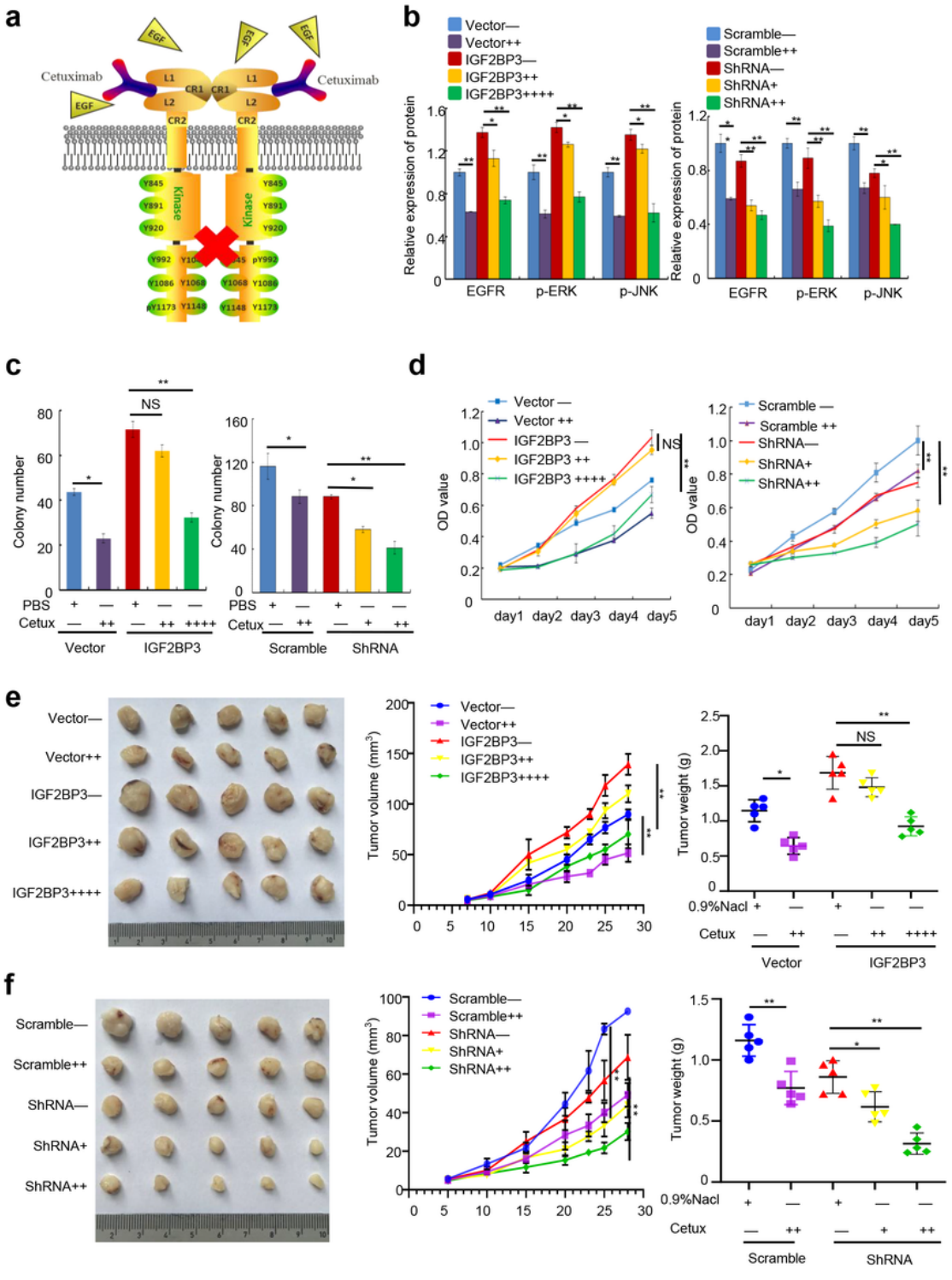

Figure 5

IGF2BP3 affects the sensitivity of CRC cells to cetuximab. **a** Cetuximab mechanism of blocking the activation of EGFR. **b** Western blot analysis and quantitation of the expression of EGFR and its

downstream effector molecules in indicated groups. **c-d** Colony formation assay (**c**) and MTT assay (**d**) validated the effect of different cetuximab treatments on the proliferation rate in indicated groups. **e-f** Representative gross images (left), tumor growth rate (middle), and tumor volume analysis (left) in mice bearing Caco2 cells in different groups and treated with different drug concentrations. n = 5. "+" represents cetuximab at a concentration of 5 μg/μl, "++" represents cetuximab at a concentration of 10 μg/μl, "++++" represents cetuximab at a concentration of 20 μg/μl Error bars represent the mean ± SD of 3 independent experiments; ns, no significance; * $p < 0.05$; ** $p < 0.01$;

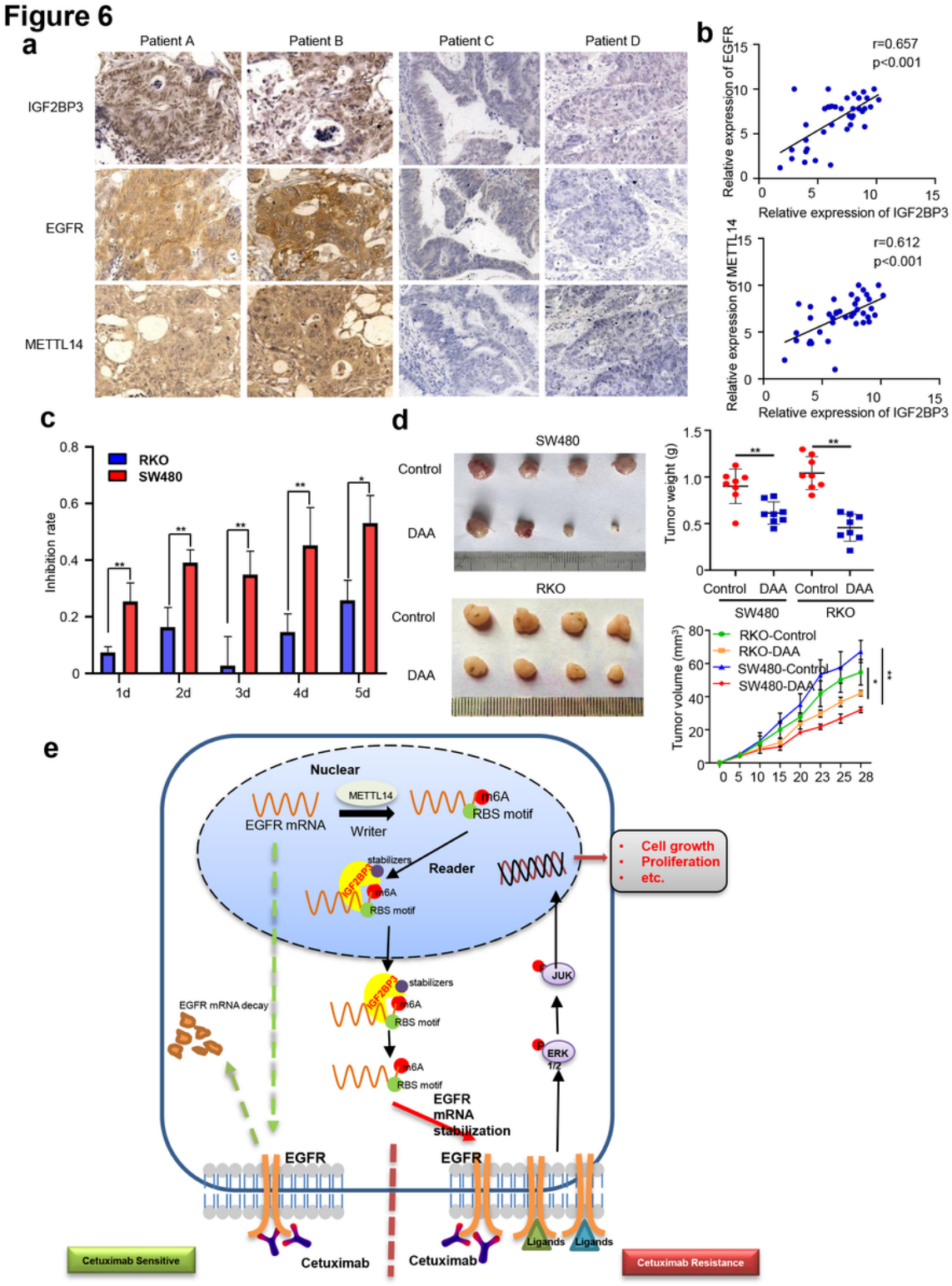

Figure 6

The level of IGF2BP3 is clinically relevant in CRC patients. **a** Representative immunohistochemical images of IGF2BP3, EGFR, and METTL14 in CRC tissues using IHC analysis. Scale bars: 50 μm (400X). **b** Correlation between IGF2BP3 expression and EGFR IHC scores in CRC tissues (up). Correlation between IGF2BP3 expression and METTL14 IHC scores in CRC tissues (down), n =40. **c** Inhibition rate of DAA (3-Deazaadenosine) (4ug/ml) in RKO and SW480 cells. **d** Representative images of tumors (left), statistical analysis of tumor volume (right) in nude mice bearing RKO or SW480 cells with or without treatment of DAA. **e** Schematic diagram of the relationship among IGF2BP3, m^6A modification, EGFR, CRC cell progression, and cetuximab resistance. Error bars represent the mean ± SD of 3 independent experiments; * $p < 0.05$; ** $p < 0.01$;

Supplementary Files

This is a list of supplementary files associated with this preprint. Click to download.

- Additionalfile1.pdf
- Additionalfile1.docx